

RESEARCH ARTICLE

10.1002/2016JA022753

This article is a companion to *Moro et al.* [2016] doi:10.1002/2016JA022751.

Key Points:

- The electric fields are more intense during summer, followed by equinox and winter in the Brazilian sector
- The electric fields are highly variable with season in the Brazilian sector compared to the Peruvian sector
- The time interval of the equatorial electrojet occurrence decreased significantly along the years in Brazil

Correspondence to:

J. Moro,
juliano.moro@inpe.br;
julianopmoro@gmail.com

Citation:

Moro, J., C. M. Denardini, L. C. A. Resende, S. S. Chen, and N. J. Schuch (2016), Equatorial E region electric fields at the dip equator: 2. Seasonal variabilities and effects over Brazil due to the secular variation of the magnetic equator, *J. Geophys. Res. Space Physics*, 121, 10,231–10,240, doi:10.1002/2016JA022753.

Received 28 MAR 2016

Accepted 20 SEP 2016

Accepted article online 23 SEP 2016

Published online 14 OCT 2016

Corrected 27 OCT 2016

This article was corrected on 27 OCT 2016. See the end of the full text for details.

Equatorial E region electric fields at the dip equator: 2. Seasonal variabilities and effects over Brazil due to the secular variation of the magnetic equator

J. Moro¹, C. M. Denardini², L. C. A. Resende², S. S. Chen^{2,3}, and N. J. Schuch¹

¹Southern Regional Space Research Center (CRS/INPE), Santa Maria, Brazil, ²National Institute for Space Research (INPE), São José dos Campos, Brazil, ³Department of Electrical Engineering, University of Taubaté, Taubaté, Brazil

Abstract In this work, the seasonal dependency of the E region electric field (EEF) at the dip equator is examined. The eastward zonal (E_y) and the daytime vertical (E_z) electric fields are responsible for the overall phenomenology of the equatorial and low-latitude ionosphere, including the equatorial electrojet (EEJ) and its plasma instability. The electric field components are studied based on long-term backscatter radars soundings (348 days for both systems) collected during geomagnetic quiet days ($Kp \leq 3+$), from 2001 to 2010, at the São Luís Space Observatory (SLZ), Brazil (2.33°S, 44.20°W), and at the Jicamarca Radio Observatory (JRO), Peru (11.95°S, 76.87°W). Among the results, we observe, for the first time, a seasonal difference between the EEF in these two sectors in South America based on coherent radar measurements. The EEF is more intense in summer at SLZ, in equinox at JRO, and has been highly variable with season in the Brazilian sector compared to the Peruvian sector. In addition, the secular variation on the geomagnetic field and its effect on the EEJ over Brazil resulted that as much farther away is the magnetic equator from SLZ, later more the EEJ is observed (10 h LT) and sooner it ends (16 h LT). Moreover, the time interval of type II occurrence decreased significantly after the year 2004, which is a clear indication that SLZ is no longer an equatorial station due to the secular variation of the geomagnetic field.

1. Introduction

The eastward zonal (E_y) electric field is generated in both daytime and nighttime atmospheric dynamos due to the neutral winds interaction with the magnetized conducting ionosphere at E layer heights. Although the E_y component is small, it is very important because it drives the vertical plasma drift. This motion is mainly responsible for the formation and structuring of the ionization layers and for the overall phenomenology of the equatorial and low-latitude ionosphere like equatorial electrojet (EEJ) and its plasma instability, the plasma fountain responsible for the equatorial ionization anomaly (EIA), and prereversal electric field enhancement (PRE) at postsunset hours leading to equatorial spread-F (ESF)/plasma bubble irregularities generation [Abdu, 2005]. Over the last several decades, extensive experimental and theoretical research have been carried out to study the diurnal, seasonal, longitudinal, latitudinal, and solar cycle variabilities of the EEJ, EIA, and ESF/plasma bubble based on the long-term ground and space-based magnetic field measurements and models [Appleton, 1946; Duncan, 1960; Hanson and Moffett, 1966; VanZandt and Peterson, 1968; Sobral et al., 1980; Kane and Trivedi, 1982; Langel et al., 1993; Chandra et al., 2000; Jadhav et al., 2002; Doumouya et al., 2003; Denardini et al., 2003, 2004, 2006, 2011, 2013, 2015; Lühr et al., 2004; Rastogi et al., 2007; Alken and Maus, 2007; Shume et al., 2011; Chandrasekhar et al., 2014].

As the São Luís Space Observatory, Brazil (SLZ, 2.33°S, 44.20°W, dip latitude: ~7°S, declination: ~21°W) and the Jicamarca Radio Observatory, Peru (JRO, 11.95°S, 76.87°W, dip latitude: ~1°N, declination: 4°E) have markedly different magnetic declination angles, certain seasonal characteristics are observed in the ionospheric phenomena between the east and west coast of South America. The E_y obtained from vertical plasma drift data measured by incoherent backscatter radar over Jicamarca, Peru, has seasonal as well as solar cycle variability, having a large magnitude during equinoxes and solar maximum conditions, as was pointed out by Fejer [1991]. This electric field is the primary element for driving the EEJ. It has often been noted that the EEJ exhibits seasonal variation in intensity, been stronger during equinox than during summer solstice, which is explained in terms of seasonal shifts of the foci of the Sq current system [Tarpley, 1973]. The Sq foci in both the Northern and Southern Hemispheres shift toward the equator during equinox (the EEJ intensity will increase) and shift toward the poles during solstice (the EEJ intensity decreases), explaining the

strengthening and weakening of the EEJ during these seasons. In the Brazilian sector, however, the EEJ has one prominent peak centering around the December and January months both during solar maximum and minimum, and the strength of the EEJ is minimum during Southern (Northern) Hemisphere winter (summer) (May–August) [Chapman and Rao, 1965; Doumouya et al., 1998; Okeke and Hamano, 2000; Denardini et al., 2005; Shume et al., 2010; Guizzelli et al., 2013]. An important factor that influences this result is certainly the large magnetic declination angle in the Brazilian sector as compared with the Peruvian sector.

The seasonal dependence of the PRE and ESF occurrence at a given longitude is also controlled by the magnetic declination angle as was pointed out by Abdu et al. [1981]. A seasonal maximum is expected when the sunset terminator aligns (moves parallel) with the magnetic meridian, which corresponds to near-simultaneous sunset of the conjugate footprints of the magnetic field lines at the E region height. Owing to the large declination angle over Fortaleza (Brazil), a required alignment is achieved during summer solstice (around December), leading to the maximum occurrence of PRE and ESF during this season. On the other hand, over Huancayo (Peru), which is a station located in a region with the magnetic declination angle close to zero, the alignment is achieved during equinox months leading to the maximum occurrence of PRE and ESF. Indeed, two maxima of ESF occurrence at Huancayo is observed, centered on the equinoctial months of September and March [Batista et al., 1986]. This evidence on the magnetic declination control of the PRE provided an important clue toward explaining the ESF seasonal pattern and its longitudinal dependence on a global basis [Abdu et al., 1992]. Maximum occurrences of plasma bubbles have also been observed in equinoctial months in some longitude sectors (Peruvian, African, and Indian) and in solstice months in the Brazilian sector [Tsunoda, 1985; Aarons, 1993; Sobral et al., 2002; Pimenta et al., 2003; Paulino et al., 2010].

In the companion paper, Moro et al. [2016b] analyzed the variabilities of the E region electric fields (EEF) in eastern coast of South America, at SLZ, and in western coast of South America, at JRO based on long term of radar soundings collected from 2001 to 2010. The authors found that, under quiet geomagnetic activity, the mean diurnal variations of E_y ranged from 0.21 to 0.35 mV/m between 8 and 18 h local time (LT) in Brazil and from 0.23 mV/m to 0.45 mV/m in Peru, while the mean diurnal variations of the E_z range from 7.09 to 8.80 mV/m in Brazil and from 9.00 to 11.18 mV/m in Peru. In this work, we use long-term backscatter radars soundings (348 days for both systems) collected under quiet geomagnetic conditions at SLZ and JRO to investigate the seasonal characteristics of the electric field components, which drive all the above mentioned phenomena (EEJ, PRE, and ESF). Moreover, we also present for the first time the impact on the EEJ due to the secular variation of the geomagnetic field over Brazil, in terms of the electric fields inferred from coherent radar data in the E region.

2. Data and Analysis

The Doppler frequency of type II echoes detected with the 50 MHz backscatter coherent radar (RESCO) set at SLZ and with the JULIA (Jicamarca Unattended Long-term Studies of the Ionosphere and Atmosphere) radar mode, which is a mode of operation of the Jicamarca radar using low power transmitters for coherent measurements, is used to infer the vertical (E_z) component of the electric field. Long-term (348 days total for both radars) soundings of RESCO and JULIA radars, collected during geomagnetic quiet days ($Kp \leq 3+$) from 2001 to 2010, are used in this study. The locations of these radars and the main systems specifications are presented in Figure 1 and Table 1 of the companion paper in this issue [Moro et al., 2016b].

The zonal electric field component, E_y , is calculated from E_z and a magnetic field line-integrated conductivity model developed by Denardini [2007] and recently updated by Moro et al. [2016a] to include more realistic atmospheric parameters. The model is essentially composed by (a) neutral densities and temperature provided by the Mass Spectrometer and Incoherent Scatter Model (NRLMSISE-00, hereafter written as MSIS), (b) electron density and ion composition in the momentum transfer collision frequency equation provided by the International Reference Ionosphere (IRI-2007) model, (c) adjustments to the mean electron density obtained from the E region ordinary frequency (f_oE) obtained by ionosondes at three stations across the magnetic equator to compensate the IRI underestimation of the E region peak density in the Brazilian sector [Abdu et al., 2004], and (d) geomagnetic field strength and its horizontal component provided by the International Geomagnetic Reference Field (IGRF-11) model.

The mean diurnal variations of the E_y and E_z at SLZ (from 2001 to 2009) and at JRO (from 2006 to 2010) are grouped into three sets, namely, equinox (March, April, September, and October), summer (November,

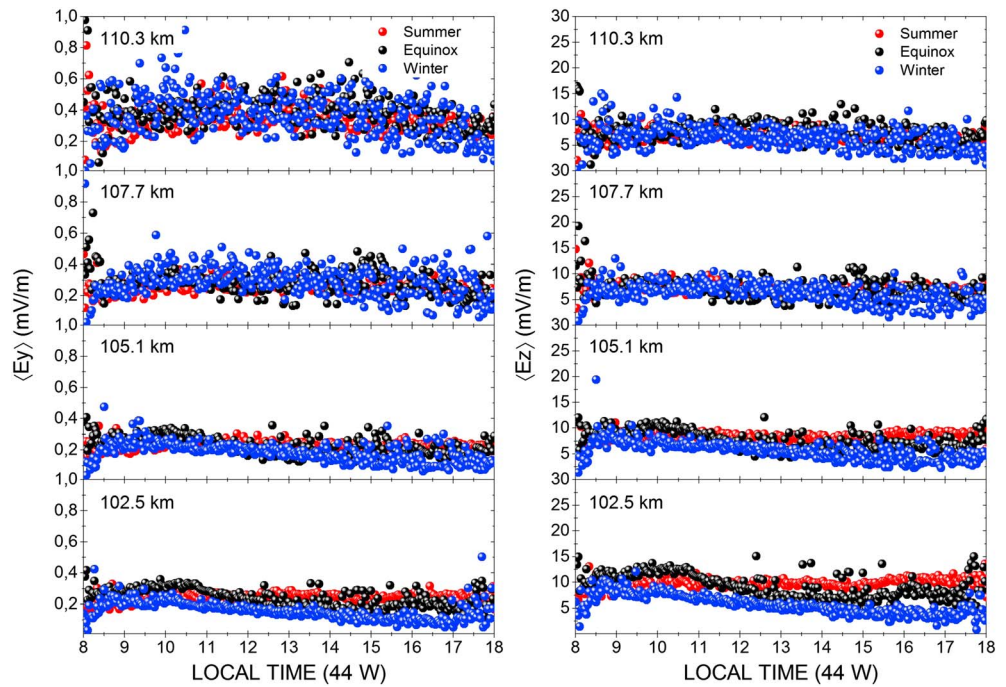


Figure 1. Mean diurnal variation of the E_y and E_z for summer (November to February: red dots), equinox (March, April, September, and October: black dots), and winter (May to August: blue dots) in Brazil.

December, January, and February), and winter (May, June, July, and August), in order to characterize the EEF seasonal variability.

3. Results and Discussions

The results of the mean diurnal variations of E_y (left) and E_z (right) per range height between 8 and 18 LT at SLZ are shown in Figure 1. The red dots represent the diurnal variation of the EEF components in summer. The black dots represent the diurnal variability in equinox, while the blue dots represent the same diurnal variation obtained in winter.

The E_y and E_z components are more intense during summer at SLZ, especially after 12 LT, in the lower EEF region (102.5 km), followed by equinox and winter. The same characteristic is observed at 105.1 km. Due to the relatively data dispersions, which makes the analysis difficult, the electric field intensities seem to have

a small seasonal dependence at 107.7 and 110.3 km. However, we can identify that E_y ranges from 0.28 to 0.97 mV/m between 8 and 18 LT in the Brazilian sector. In regard to E_z , it ranges from 0.24 to 19.42 mV/m.

Table 1. Daily Average of $\langle E_y \rangle$ (mV/m) and $\langle E_z \rangle$ (mV/m) and Corresponding Standard Deviation per RESCO Range Height and Seasons at SLZ

Season	Height (km)	$\langle E_y \rangle \pm \langle SD \rangle$	$\langle E_z \rangle \pm \langle SD \rangle$
Summer	110.3	0.33 ± 0.08	6.96 ± 1.08
	107.7	0.26 ± 0.03	7.22 ± 0.92
	105.1	0.24 ± 0.02	9.76 ± 0.97
	102.5	0.24 ± 0.02	8.39 ± 0.77
Equinox	110.3	0.39 ± 0.10	7.50 ± 1.90
	107.7	0.29 ± 0.07	7.11 ± 1.78
	105.1	0.22 ± 0.05	9.25 ± 2.35
	102.5	0.23 ± 0.06	7.55 ± 1.78
Winter	110.3	0.36 ± 0.14	6.44 ± 2.25
	107.7	0.29 ± 0.10	6.37 ± 2.38
	105.1	0.18 ± 0.06	5.68 ± 1.89
	102.5	0.15 ± 0.05	5.63 ± 1.80

The results of the diurnal variations of E_y (left) and E_z (right) per range height between 8 and 18 LT at JRO are shown in Figure 2. The figure follows the same pattern of Figure 1, i.e., the red dots represent the diurnal variation of the EEF components in summer. The black dots represent the diurnal variability in equinox, while the blue dots represent the same diurnal

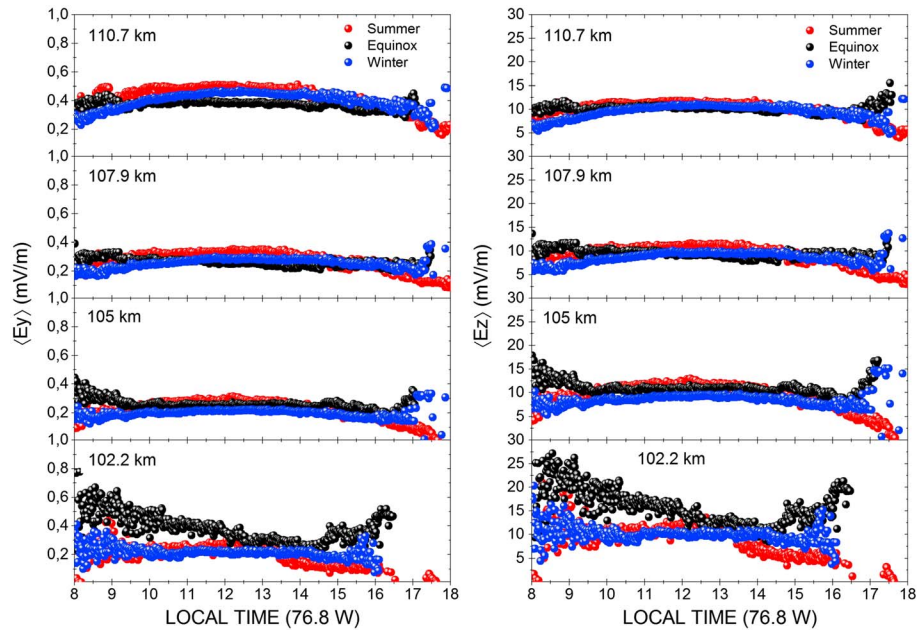


Figure 2. Mean diurnal variation of the E_y and E_z for summer (November to February: red dots), equinox (March, April, September, and October: black dots), and winter (May to August: blue dots) in Peru.

variation obtained in winter. Contrary to the mean diurnal variations of the E_y and E_z inferred at SLZ, in Figure 2 we observe strong data dispersion between 8 and 10 LT and after 15 LT at 102.2 km in both components. After this variability, there is a tendency of the EEF to stabilize between 10 and 15 LT at 102.2 km and above 105.0 km. The type II irregularities were not observed at JRO by the end of the measurement period (after 17 LT) at 102 km in equinox and winter seasons. Consequently, no EEF was inferred. Also, the EEF starts to decrease after 17 LT in summer in all range heights, whereas the EEF starts to be more intense during equinox and winter seasons, which is still a matter of study. Figure 2 also shows that E_y ranges from 0.071 to 0.77 mV/m between 8 and 18 LT in the Peruvian sector. In regard to the E_z , it ranges from 0.72 to 27.18 mV/m. This indicates that E_z is characterized to be more intense at JRO than at SLZ. We also could have the same conclusion for the E_y variability since the maximum value at SLZ (0.97 mV/m) is just an isolated value in the data at 110.3 km in equinox.

We also calculated the daily average of E_y (i.e., $\langle E_y \rangle$) and the daily average of E_z (i.e., $\langle E_z \rangle$) and their standard deviations in order to further investigate the height dependence of the mean EEF seasonal variability between both sectors. These average values are presented in the vertical profiles in Figure 3, and the specific values are listed in Table 1 for SLZ and Table 2 for JRO.

The first characteristic shown in Figure 3 to be discussed here is the gradients in E_y and E_z in both sectors. A positive gradient with height is observed in summer and winter for $\langle E_y \rangle$ and only in winter for $\langle E_z \rangle$ at SLZ. This characteristic is also observed only in summer for both components at JRO. During equinox, $\langle E_y \rangle$ is slightly higher at 102.5 km than at 105.1 km at SLZ and JRO. With respect to the electric field intensities between the seasons in the same component and observatory, Table 1 shows that E_y and E_z are more intense in the lower EEJ region during summer, followed by equinox and winter in the Brazilian sector. The higher $\langle E_y \rangle$ (0.39 mV/m) is found at 110.3 km in equinox at SLZ, while the lower $\langle E_y \rangle$ (0.15 mV/m) is found at 102.5 km during winter. The higher $\langle E_z \rangle$ (9.76 mV/m) is found in the central region of the EEJ in summer, and the lower $\langle E_z \rangle$ (5.63 mV/m) is found at 102.5 km in winter. Table 2 shows that E_y and E_z are more intense during equinox in the Peruvian sector. Indeed, in the lower EEJ region, below ~ 108 km, E_y is pretty much the same in summer and winter. The higher $\langle E_y \rangle$ (0.39 mV/m) is found at 110.7 km at JRO, while the lower $\langle E_y \rangle$ (0.19 mV/m) is found at 105.0 km, both in winter. Table 2 also shows that the higher $\langle E_z \rangle$ (12.69 mV/m) is found at 102.2 km in equinox, while the lower $\langle E_z \rangle$ (8.39 mV/m) is found at 105.0 km during winter.

In Figure 3, we can see similarities in E_y and dissimilarities in E_z when we analyze the electric fields between the two longitudinal sectors in the same season. Figures 3a–3c show that the E_y values are pretty close in the

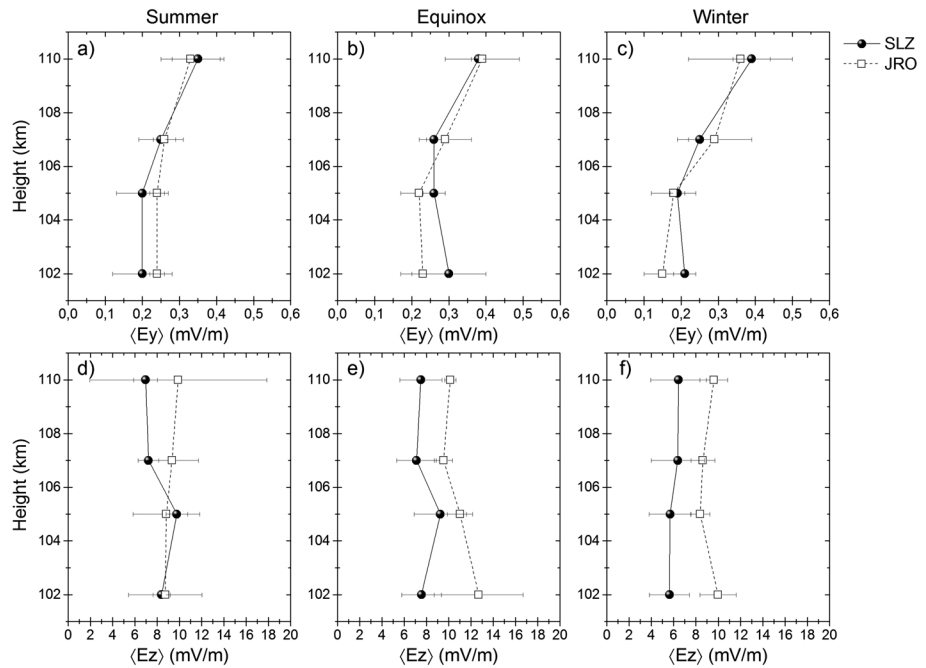


Figure 3. Vertical profiles of (a–c) $\langle E_y \rangle$ and (d–f) $\langle E_z \rangle$ estimate during summer, equinox, and winter at the São Luís Space Observatory, Brazil (SLZ, dots with solid lines), and at the Jicamarca Radio Observatory, Peru (JRO, squares with dashed lines).

four ranges of radar heights, in the same season, in both sectors. However, there is a clear difference in E_z during the equinox, Figure 3e, and winter, Figure 3f, between SLZ and JRO. The E_z component is more intense in the four ranges of radar heights at JRO. During summer, Figure 3d, E_z is also more intense in three out of four heights. In addition, the EEF is highly variable with season at SLZ compared to JRO, as we can see by the standard deviations in Tables 1 and 2. For the first time based on the EEF inference, a clear seasonal difference between the electric fields in two sectors in South America is shown. This result explains and gives support to several characteristics observed in previous studies related to the seasonal characteristics of the EEJ, EIA, and ESF/plasma bubble irregularities in Brazil and Peru.

Despite that the electric fields are estimated in the E region, they influence the F region, since the E region dynamo fields are coupled to the F region through the equipotential magnetic field lines. Consequently, the equatorial zonal and vertical drifts are driven, respectively, by the E_z and E_y along a magnetic flux tube. Such behavior was first reported in the evening PRE enhancements in the Brazilian sector by *Abdu et al.* [1981], which presented the monthly mean variations of vertical F layer velocities (V_z) deduced from nighttime ionograms and observed profound differences in the seasonal trends in the times and widths of V_z over

Table 2. Daily Average of $\langle E_y \rangle$ (mV/m) and $\langle E_z \rangle$ (mV/m) and Corresponding Standard Deviation per JULIA Range Height and Seasons at the JRO

Season	Height (km)	$\langle E_y \rangle \pm \langle SD \rangle$	$\langle E_z \rangle \pm \langle SD \rangle$
Summer	110.7	0.35 ± 0.07	9.59 ± 1.95
	107.9	0.25 ± 0.06	9.34 ± 2.37
	105.0	0.20 ± 0.07	8.83 ± 3.01
	102.2	0.20 ± 0.08	8.73 ± 3.30
Equinox	110.7	0.38 ± 0.02	10.14 ± 0.52
	107.9	0.26 ± 0.02	9.53 ± 0.81
	105.0	0.26 ± 0.03	11.02 ± 1.13
	102.2	0.30 ± 0.10	12.69 ± 4.00
Winter	110.7	0.39 ± 0.05	9.61 ± 1.24
	107.9	0.25 ± 0.03	8.62 ± 1.07
	105.0	0.19 ± 0.02	8.39 ± 0.85
	102.2	0.21 ± 0.03	9.98 ± 1.62

Fortaleza (4°S, 38°W, Brazil) and Jicamarca. As mentioned by *Abdu et al.* [1981], the dissimilarities are shown to be arising mainly from the difference in the magnetic field declination angles between the two observatories. As a result, sunset durations at the conjugate footprints of the magnetic field lines at the E region height are different leading to differences in the F region polarization electric field development rates at the two observatories. In a more recent work, *Denardini et al.* [2005] have studied the seasonal characteristics of the EEJ observed over SLZ based on a 1 year data set collected by the RESCO radar. The mean Range Time Intensity (RTI) maps for summer, equinoxes, and winter obtained for the quiet period (please see Figure 1 in their work) clearly show that the EEJ power echo is stronger during summer, and weaker echoes are observed during winter, which indicates the characteristics discussed in this work (see $\langle E_z \rangle$ in Table 1). *Denardini et al.* [2005] did not conduct a comparison study with Jicamarca, although. *Shume et al.* [2010] presented the variabilities of the EEJ in Brazil and Peru and spectrally analyzed the ΔH magnetic field perturbation measurements with wavelet, and they clearly show that the EEJ has maxima around equinoxes in JRO and during summer at SLZ, which also corroborates with the characteristics observed in this work (see $\langle E_z \rangle$ in Table 2). The results of *Shume et al.* [2010] were explained in terms of the magnetic declination angle difference between the two sectors. Moreover, *Guizelli et al.* [2013] presented that the EEJ plasma irregularities are most common in equinox and less in summer at the JRO, based on a seasonal statistical study of the occurrence of EEJ plasma irregularities at JRO covering 2 years of data (2007 and 2008).

Regarding the differences in the EEJ patterns that have been observed between SLZ and JRO, which cause the seasonal differences in ionospheric phenomena reported previously, we may state that they are due to the position of the dip equator vis à vis the geographic equator between these two observatories. It is well known from observations of the magnetic field that the pattern of the declination seen at the Earth's surface appears to be moving slowly westward and mainly apparent in the east coast of Brazil at middle and equatorial latitudes. This is related to the motion of fluid at the core surface slowly westward, dragging with it the geomagnetic field, and so the geographic locus where the EEJ is formed.

In order to analyze the secular variation of the geomagnetic field and its effect on the EEJ and electric fields over Brazil, we present a map built from the E_z component inferred from eight probe data (1 day per year between 2001 and 2009, except of year 2008) obtained from the RESCO radar in Figure 4. The data were acquired in days with similar geophysical conditions (or as closely as possible). The vertical axis gives the years in which the E_z component was derived, and the horizontal axis gives the corresponding local time of the RESCO soundings (44 W). The color scale on the right of the fourth panel shows the intensity of E_z with a maximum of 24 mV/m. The white portions correspond the time interval with no type II detection during the radar operation. This figure allows us to analyze the effects in the EEJ as a function of the increasing distance of SLZ from the center of EEJ during the 8 year period, since the E_z component is responsible for the gradient $E \times B$ drift instability process that manifests as type II irregularities in radar data, and it is expected to weaken at distances away from the EEJ center.

Figure 4 shows that the higher E_z intensities occurred from 8 to 18 LT in 2002 and from ~0930 to ~15 LT in 2005, in the lower EEJ region (102.5 km). The E_z intensity decreased as height increased. The type II irregularities had a significant delay to develop (~1 h) and ceased before 18 LT after the year 2003. This is a clear characteristic after the year 2004, which is an indication of the geomagnetic equator displacement over the SLZ region. As the geomagnetic field structure, centered at the dip equator, undergoes a steady northwestward excursion causing variation in the EEJ observed on the ground, the radar started to operate from 9 to 18 LT after 2008. Finally, the EEJ developed after 10 LT and vanished before 16 LT in 2009. Thus, the main point that comes out of the present analysis is that as much farther away is the dip equator from SLZ, later more the EEJ is observed (10 LT) and sooner it ends (16 LT), the first ever result showing this relationship. It should be noted that the radar operated between 8 and 18 LT every single day up to 2007.

As the dayside EEJ is a current sheet flowing eastward along the geomagnetic dip latitudes (usually mentioned to be around $\pm 3^\circ$) at 105 km altitude, and once SLZ reached this threshold in 2003, we were surprised that the EEJ irregularities were detected during the time interval of the EEJ occurrence long after that, even if significantly decreased due to the secular variation of the dip equator over Brazil.

Besides the effects in the EEJ, the displacement of the geomagnetic equator may affect the sporadic E (E_s) layers over SLZ. However, the presence of very strong (in signal-to-noise terms) EEJ makes it difficult to observe E_s layers with radar echoes. Indeed, the first observations of E_s layers with radar, as far as we know,

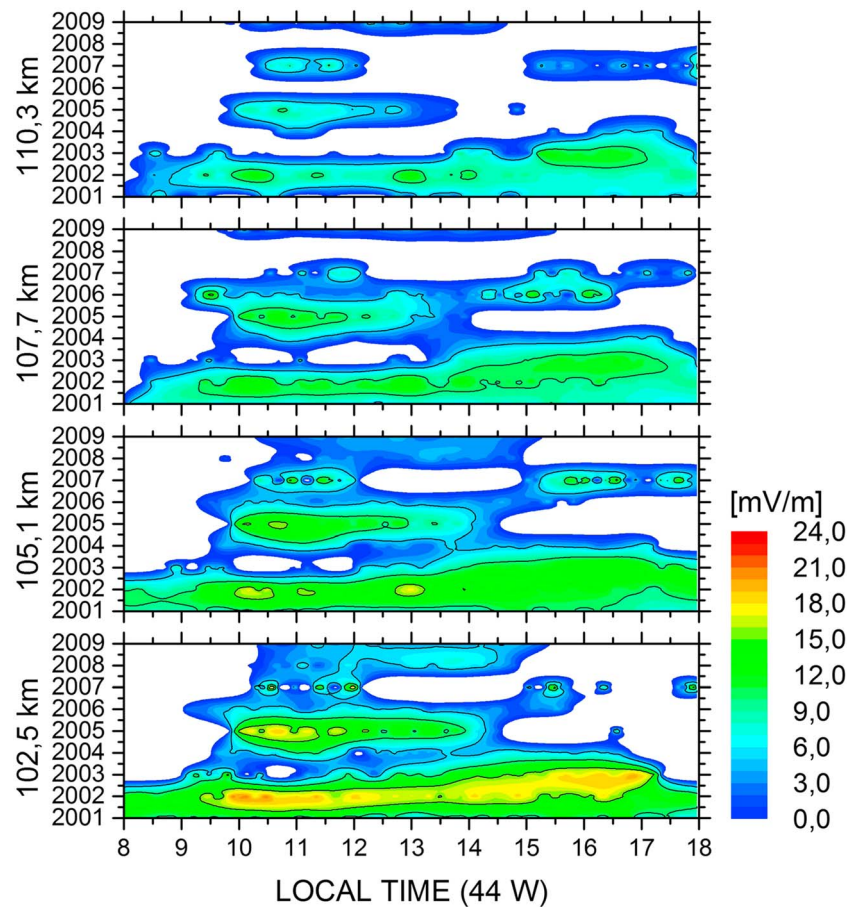


Figure 4. E_z map built from a single day per year, for the same season and local time, at four distinct range heights of RESCO observations from 2001 to 2009.

were made by *Malhotra et al.* [2008] using the Jicamarca radar. The E_s layers, as observed from ionosonde measurements, have been classified into several types according to the different mechanisms of formation and location at which they are observed. The well-known gradient drift mechanism is known to be responsible for the equatorial-type sporadic E layer (E_{sq}) that occurs inside the EEJ, whereas other different types of blanketing E_s layers (E_{sb} labeled as "h" and "c") occur at low latitudes, in the vicinity of the EEJ, and are known to be produced by wind shear mechanism [Axford, 1963; Whitehead, 1961; Haldoupis, 2011]. The signature of the E_{sq} appears in ionograms as a scattering of the radio signal that covers most frequencies during the daytime. With the displacement of the geomagnetic equator over SLZ, a decrease (increase) in the occurrence rates of the E_{sq} (E_{sb}) is expected.

A recent study [Resende, 2014] of the competition between tidal winds and electric fields in the formation of E_{sb} over SLZ reported an increase in the occurrence rates of E_{sb} since 2009, revealing that the EEJ has few or no influence at SLZ. In addition, the E_{sb} layers are frequently observed from this year to now. Moreover, during a geomagnetically disturbed period during the solar cycle 23, Resende et al. [2013] observed different types of E_{sb} layers that were mainly associated with the displacement of the magnetic equator in relation to SLZ. A systematic decrease in the occurrence rates of the E_{sq} was observed at Fortaleza, a station where the secular variation of the geomagnetic field has caused a steady drift of the magnetic equator to north of the station since 1975. Abdu et al. [1996] observed that the E_{sq} decreased from ~90% occurrence in 1975 to almost insignificant value around 1989, period which the magnetic equator drifted northward of Fortaleza by 400 km. On the other hand, the h and c types of E_{sb} layers showed significant enhancements toward 1989 suggesting that their occurrence increased with increasing distance of Fortaleza from the EEJ center. This characteristic has not been observed at Jicamarca yet, since the magnetic equator is not moving away over JRO in such rate as observed at SLZ.

4. Summary and Conclusions

This work presents the seasonal variabilities of the E region electric fields (EEF) in Brazil (São Luís Space Observatory—SLZ, 2.33°S, 44.20°W) and Peru (Jicamarca Radio Observatory—JRO, 11.95°S, 76.87°W). The vertical (E_z) electric field component is inferred from the Doppler shifts of type II echoes detected with the RESCO and JULIA coherent backscatter radars during the solar cycles 23 and 24. The eastward zonal (E_y) electric field component is obtained from the E_z and the Hall-to-Pedersen ionospheric conductivity ratio. The mean diurnal variations of E_y and E_z , inferred from long term (348 days for both systems) of radar soundings collected during geomagnetic quiet days ($Kp \leq 3+$) from 2001 to 2010, are grouped into three sets, namely, equinox (March, April, September, and October), summer (November, December, January, and February), and winter (May, June, July, and August) in order to characterize the EEF seasonal variability.

We observe a strong data dispersion in E_y at 110.3 km and a more stable characteristic in the other range heights and in the E_z component at SLZ. The EEF components are more intense during summer, especially after 12 LT in the lower EEJ region, followed by equinox and winter. Above 107 km we are not able to clearly identify the seasonal influence in E_y at SLZ. The E_y component ranges from 0.28 to 0.97 mV/m between 8 and 18 LT in the Brazilian sector, and the E_z component ranges from 0.24 to 19.42 mV/m. Both E_y and E_z components inferred at JRO show strong data dispersion between 8 and 10 h and after 15 h at 102.2 km. This characteristic stabilizes between 10 and 15 h at 102.2 km and above 105.0 km. The EEF components start to decrease after 17 h in the summer in all range heights, which is still a matter of study. The E_y component ranges from 0.071 to 0.77 mV/m between 8 and 18 h, and E_z ranges from 0.72 to 27.18 mV/m in the Peruvian sector. This indicates that E_z is characterized to be more intense at JRO than at SLZ. Moreover, the EEF is highly variable with season at SLZ compared to JRO. The geomagnetic field secular variations in the South America are moving fast enough to cause changes in the EEF that can be observed in the time scale of a solar cycle or less. This is the case with the Brazilian longitude sector where the rate of secular variations is the fastest over the low-latitude region of the globe. The E_z map, built from a single day per year between 2001 and 2009 (exception of year 2008), shows that after the year 2003 the type II irregularities had some delay to develop especially above 105 km, and the irregularities ceased before 18 h. This characteristic is cleared from the year 2004. The EEJ developed after 10 h and vanished before 16 h in 2009, indicating that the time interval of its occurrence decreased significantly.

Acknowledgments

J. Moro thanks CNPq/MCTIC (grant 312775/2015-6) and the National Space Science Center (NSSC), Chinese Academy of Sciences (CAS) for supporting his postdoctoral. C.M. Denardini thanks CNPq/MCTIC (grant 303121/2014-9) and FAPESP (grant 2012/08445-9). L.C.A. Resende thanks FAPESP (grant 2014/11198-9). S.S. Chen thanks CNPq/MCTIC (grant 312730/2015-2). The authors thank DAE/INPE for kindly providing the RESCO data. Clezio M. Denardini is responsible for the RESCO data, e-mail: clezio.denardin@inpe.br. The Jicamarca Radio Observatory is gratefully acknowledged for providing the JULIA data. The Jicamarca Radio Observatory is a facility of the Instituto Geofísico del Peru operated with support from the NSF AGS-1433968 through Cornell University (request data by emailing databasejro.igp.gob.pe). The authors wish to acknowledge the Editor and referees for their assistance in evaluating this paper.

References

- Aarons, J. (1993), The longitudinal morphology of equatorial F layer irregularities relevant to their occurrence, *Space Sci. Rev.*, *63*, 209–243, doi:10.1007/BF00750769.
- Abdu, M. A. (2005), Outstanding problems in the equatorial ionosphere-thermosphere electrodynamic relevant to spread F, *J. Atmos. Sol. Terr. Phys.*, *63*, 869–884, doi:10.1016/S1364-6826(00)00201-7.
- Abdu, M. A., J. A. Bittencourt, and I. S. Batista (1981), Magnetic declination control of the equatorial F region dynamo electric field development and spread F, *J. Geophys. Res.*, *86*, 11,443–11,446, doi:10.1029/JA086iA13p11443.
- Abdu, M. A., I. S. Batista, and J. H. Sobral (1992), A new aspect of magnetic declination control of equatorial spread F and F region dynamo, *J. Geophys. Res.*, *97*, 14,897–14,904, doi:10.1029/92JA00826.
- Abdu, M. A., I. S. Batista, P. Muralikrishna, and J. H. A. Sobral (1996), Long term trends in sporadic E layers and electric fields over Fortaleza, Brazil, *Geophys. Res. Lett.*, *23*, 757–760, doi:10.1029/96GL00589.
- Abdu, M. A., I. S. Batista, B. W. Reinisch, and A. J. Carrasco (2004), Equatorial F-layer heights, evening prereversal electric field, and night E-layer density in the American sector: IRI validation with observations, *Adv. Space Res.*, *34*(9), 1953–1965, doi:10.1016/j.asr.2004.04.011.
- Alken, P., and S. Maus (2007), Spatio-temporal characterization of the equatorial electrojet from CHAMP, Ørsted, and SAC-C satellite magnetic measurements, *J. Geophys. Res.*, *112*, A09305, doi:10.1029/2007JA012524.
- Appleton, E. V. (1946), Two anomalies in the ionosphere, *Nature*, *157*, 691–693, doi:10.1038/157691a0.
- Axford, W. I. (1963), The formation and vertical movements of dense ionized layers in the ionosphere due to neutral wind shears, *J. Geophys. Res.*, *68*, 769–779, doi:10.1029/JZ068i003p00769.
- Batista, I. S., M. A. Abdu, and J. A. Bittencourt (1986), Equatorial F region vertical plasma drifts: Seasonal and longitudinal asymmetries in the American sector, *J. Geophys. Res.*, *91*, 12,055–12,064, doi:10.1029/JA091iA11p12055.
- Chandra, H., H. S. S. Sinha, and R. G. Rastogi (2000), Equatorial electrojet studies from rocket and ground measurements, *Earth Planets Space*, *52*, 111–120, doi:10.1186/BF03351619.
- Chandrasekhar, N. P., K. Arora, and N. Nagarajan (2014), Characterization of seasonal and longitudinal variability of EEJ in the Indian region, *J. Geophys. Res. Space Physics*, *119*, 10,242–10,259, doi:10.1002/2014JA020183.
- Chapman, S., and K. S. R. Rao (1965), The H and Z variations along and near the equatorial electrojet in India, Africa, and the Pacific, *J. Atmos. Terr. Phys.*, *27*, 559–581, doi:10.1016/0021-9169(65)90020-6.
- Denardini, C. M. (2007), A conductivity model for the Brazilian equatorial E-region: Initial results, *Braz. J. Geophys.*, *25*(2), 87–94.
- Denardini, C. M., M. A. Abdu, and J. H. A. Sobral (2003), Detection of three distinct regions in the equatorial electrojet in the Brazilian sector, *Braz. J. Geophys.*, *21*(1), 65–74.

- Denardini, C. M., M. A. Abdu, and J. H. A. Sobral (2004), VHF radar studies of the equatorial electrojet 3-m irregularities over Sao Luis: Day-to-day variabilities under auroral activity and quiet conditions, *J. Atmos. Sol. Terr. Phys.*, *66*(17), 1603–1613, doi:10.1016/j.jastp.2004.07.031.
- Denardini, C. M., M. A. Abdu, E. R. de Paula, J. H. A. Sobral, and C. M. Wrasse (2005), Seasonal characterization of the equatorial electrojet height rise over Brazil as observed by the RESCO 50 MHz back-scatter radar, *J. Atmos. Sol. Terr. Phys.*, *67*(17–18), 1665–1673, doi:10.1016/j.jastp.2005.04.008.
- Denardini, C. M., M. A. Abdu, E. R. de Paula, C. M. Wrasse, and J. H. A. Sobral (2006), VHF radar observations of the dip equatorial E-region during sunset in the Brazilian sector, *Ann. Geophys.*, *24*(6), 1617–1623, doi:10.5194/angeo-24-1617-2006.
- Denardini, C. M., H. C. Aveiro, P. D. S. C. Almeida, L. C. A. Resende, L. M. Guizelli, J. Moro, J. H. A. Sobral, and M. A. Abdu (2011), Daytime efficiency and characteristic time scale of interplanetary electric fields penetration to equatorial latitude ionosphere, *J. Atmos. Sol. Terr. Phys.*, *73*(11–12), 1555–1559, doi:10.1016/j.jastp.2010.09.003.
- Denardini, C. M., H. C. Aveiro, J. H. A. Sobral, J. V. Bageston, L. M. Guizelli, L. C. A. Resende, and J. Moro (2013), E region electric fields at the dip equator and anomalous conductivity effects, *Adv. Space Res.*, *51*(10), 1857–1869, doi:10.1016/j.asr.2012.06.003.
- Denardini, C. M., J. Moro, L. C. A. Resende, S. S. Chen, N. J. Schuch, and J. E. R. Costa (2015), E region electric field dependence of the solar activity, *J. Geophys. Res. Space Physics*, *120*, 8934–8941, doi:10.1002/2015JA021714.
- Doumouya, V., J. Vassel, Y. Cohen, O. Fambitakoye, and M. Menvielle (1998), Equatorial electrojet at African longitudes: First results from magnetic measurements, *Ann. Geophys.*, *16*, 658–676, doi:10.1007/s00585-998-0658-9.
- Doumouya, V., Y. Cohen, B. R. Arora, and K. Yumoto (2003), Local time and longitude dependence of the equatorial electrojet magnetic effects, *J. Atmos. Sol. Terr. Phys.*, *65*, 1265–1282, doi:10.1016/j.jastp.2003.08.014.
- Duncan, R. A. (1960), The equatorial F region of the ionosphere, *J. Atmos. Sol. Terr. Phys.*, *18*, 89, doi:10.1016/0021-9169(60)90081-7.
- Fejer, B. G. (1991), Low latitude electrodynamic plasma drifts: A review, *J. Atmos. Sol. Terr. Phys.*, *53*(8), 677–693, doi:10.1016/0021-9169(91)90121-M.
- Guizelli, L. M., C. M. Denardini, J. Moro, and L. C. A. Resende (2013), Climatological study of the daytime occurrence of the 3-meter EEE plasma irregularities over Jicamarca close to the solar minimum (2007 and 2008), *Earth Planets Space*, *65*(1), 39–44, doi:10.5047/eps.2012.05.008.
- Haldoupis, C. (2011), A tutorial review on sporadic E layers, in *Aeronomy of the Earth's Atmosphere-Ionosphere*, IAGA Book Ser., vol. 2, chap. 29, pp. 381–394, Springer, Dordrecht, Netherlands, doi:10.1007/978-94-007-0326-1_29.
- Hanson, W. B., and R. J. Moffett (1966), Ionization transport effects in the equatorial F region, *J. Geophys. Res.*, *71*, 5559–5572, doi:10.1029/JZ071i023p05559.
- Jadhav, G., M. Rajaram, and R. Rajaram (2002), A detailed study of equatorial electrojet phenomena using Ørsted satellite observations, *J. Geophys. Res.*, *107*(A8), 1175, doi:10.1029/2001JA000183.
- Kane, R. P., and N. B. Trivedi (1982), Comparison of equatorial electrojet characteristics at Huancayo and Eusebio (Fortaleza) in the south American region, *J. Atmos. Sol. Terr. Phys.*, *44*, 785–792, doi:10.1016/0021-9169(82)90007-1.
- Langel, R. A., M. Pucker, and M. Rajaram (1993), The equatorial electrojet and associated currents as seen in Magsat data, *J. Atmos. Sol. Terr. Phys.*, *55*, 1233–1269, doi:10.1016/0021-9169(93)90050-9.
- Lühr, H., S. Maus, and M. Rother (2004), Noontime equatorial electrojet: Its spatial features as determined by the CHAMP satellite, *J. Geophys. Res.*, *109*, A01306, doi:10.1029/2002JA009656.
- Malhotra, A., J. D. Mathews, and J. Urbina (2008), Effect of meteor ionization on sporadic-E observed at Jicamarca, *Geophys. Res. Lett.*, *35*, L15106, doi:10.1029/2008GL034661.
- Moro, J. M., C. M. Denardini, L. C. A. Resende, S. S. Chen, and N. J. Schuch (2016a), Influence of uncertainties of the empirical models for inferring the E-region electric fields at the dip equator, *Earth Planets Space*, doi:10.1186/s40623-016-0479-0.
- Moro, J. M., C. M. Denardini, L. C. A. Resende, S. S. Chen, and N. J. Schuch (2016b), Equatorial E-region electric fields at the dip equator: 1. Variabilities in east Brazil and Peru, *J. Geophys. Res. Space Physics*, doi:10.1002/2016JA022751.
- Okeke, F. N., and Y. Hamano (2000), Daily variations of geomagnetic H, D, and Z field at equatorial latitudes, *Earth Planets Space*, *52*, 237–243, doi:10.1186/BF03351632.
- Paulino, I., A. F. Medeiros, R. A. Buriti, H. Takahashi, J. H. A. Sobral, and D. Gobbi (2010), Optical observations of east–west plasma bubble zonal drifts, *J. Atmos. Sol. Terr. Phys.*, *72*(5–6), 521–527, doi:10.1016/j.jastp.2010.01.015.
- Pimenta, A. A., P. R. Fagundes, Y. Sahai, J. A. Bittencourt, and J. R. Abalde (2003), Equatorial F-region plasma depletion drifts: Latitudinal and seasonal variations, *Ann. Geophys.*, *21*(12), 2315–2322, doi:10.5194/angeo-21-2315-2003.
- Rastogi, R. G., H. Chandra, D. Chakrabarty, K. Kitamura, and K. Yumoto (2007), Day-to-day variability of the equatorial electrojet current in the South American sector, *Earth Planets Space*, *59*, 459–461, doi:10.1186/BF03352707.
- Resende, L. C. A. (2014), Study about the formation and dominance of the sporadic E layers considering the competition between winds and electric fields, Doctoral Dissertation, Natl. Inst. for Space Res. [Available at <http://mtc-m21b.sid.inpe.br/col/sid.inpe.br/mtc-m21b/2014/09.23.20.10/doc/publicacao.pdf>].
- Resende, L. C. A., C. M. Denardini, and I. S. Batista (2013), Abnormal fbEs enhancements in equatorial Es layers during magnetic storms of solar cycle 23, *J. Atmos. Sol. Terr. Phys.*, *102*, 228–234, doi:10.1016/j.jastp.2013.05.020.
- Shume, E. B., C. M. Denardini, E. R. de Paula, and N. B. Trivedi (2010), Variabilities of the equatorial electrojet in Brazil and Perú, *J. Geophys. Res.*, *115*, A06306, doi:10.1029/2009JA014984.
- Shume, E. B., E. R. de Paula, E. A. Kherani, M. A. Abdu, and C. M. Denardini (2011), Equatorial electrojet plasma irregularities observed during late afternoon by the 30 MHz coherent scatter radar in São Luís, Brazil, *J. Atmos. Sol. Terr. Phys.*, *73*, 1560–1567, doi:10.1016/j.jastp.2011.02.015.
- Sobral, J. H. A., M. A. Abdu, I. S. Batista, and C. J. Zamlutti (1980), Association between plasma bubble irregularities and airglow disturbances over Brazilian low latitudes, *Geophys. Res. Lett.*, *11*, 980–982, doi:10.1029/GL007i011p00980.
- Sobral, J. H. A., M. A. Abdu, H. Takahashi, M. J. Taylor, E. R. de Paula, C. J. Zamlutti, M. G. D. Aquino, and G. L. Borba (2002), Ionospheric plasma bubble climatology over Brazil based on 22 years (1977–1998) of 630 nm airglow observations, *J. Atmos. Sol. Terr. Phys.*, *64*, 1517–1524, doi:10.1016/S1364-6826(02)00089-5.
- Tarpley, J. D. (1973), Seasonal movement of the Sq current foci and related effects in the equatorial electrojet, *J. Atmos. Sol. Terr. Phys.*, *35*, 1063–1071, doi:10.1016/0021-9169(73)90005-6.
- Tsunoda, R. T. (1985), Control of the seasonal and longitudinal occurrence of equatorial scintillation by longitudinal gradient in integrated Pedersen conductivity, *J. Geophys. Res.*, *90*, 447–456, doi:10.1029/JA090iA01p00447.
- VanZandt, T. E., and V. L. Peterson (1968), Detailed maps of tropical nightglow enhancements and their implications on the ionospheric F2 Layer, *Ann. Geophys.*, *24*(3), 747–749.
- Whitehead, J. D. (1961), The formation of the sporadic-E layer in the temperate zone, *J. Atmos. Sol. Terr. Phys.*, *20*, 49–58, doi:10.1016/0021-9169(61)90097-6.

Erratum

The Acknowledgment statement in the originally published article was incomplete. This version contains all necessary acknowledgments and may be considered the final version of record.